Population variability and temporal disorder disrupt coherent motion and biological functionality of active matter

M. Leoni[1,2] and T. B. Liverpool [3]
[1] *Institut Curie, PSL, 26 Rue d'Ulm, 75005, Paris*
[2] *Physics Department, Syracuse University, Syracuse, NY 13244, USA.*
[3] *School of Mathematics, University of Bristol, Bristol BS8 1TW, U.K. and BrisSynBio, Life Sciences Building, University of Bristol, Tyndall Avenue, Bristol BS8 1TQ, UK*
(Dated: October 30, 2018)

We study the effect of population variability on the collective dynamics of interacting cyclic active elements, modeled as oscillators whose frequencies are a sum of a deterministic part, identical for all elements, and a random part. The random part can vary both in amplitude and over time yielding quenched or annealed temporal disorder, as well as an intermediate regime where the noise varies over a timescale comparable to the period. In the absence of randomness, the elements synchronize in-phase and spontaneous coherent motion emerges. However, if the population variability is large enough, then synchronization is lost. This transition to a non-synchronized state is governed by properties of the tail of the population distribution that can be understood by an analysis of the properties of a random matrix. We find that collections of elements with annealed temporal disorder can tolerate, remaining functional (i.e. synchronized), higher levels of variability than the quenched cases. This is essential for identifying the design constraints of functional synthetic biological systems in the presence of unavoidable disorder.

A variety of cellular and sub-cellular processes in biology depend on non-equilibrium, active, forces cyclically varying in *space* and *time*. Such phenomena emerge in assemblies of motor proteins [? ? ?] and in assemblies of cilia and flagella [?]. Cytoskeletal organization at cell leading edges [?], which contribute to the motility of cells and cell fragments [?], involves cycles of protrusion, adhesion and retraction [?]. Noisy cell shape oscillations [? ?] and oscillating traction forces are seen at subcellular [?] and cellular [?] scale. On larger scales, inside cell monolayers, the volume of individual cells fluctuates in space and time [?] and pulsatile activity of the cytoskeleton takes place also at larger scales during embryo development [?].

Active matter [? ? ?] studies the non-equilibrium dynamics of self-driven particles [?] which can interact with each other [? ? ? ? ? ?]. It has been proposed as a novel conceptual framework to model the dynamics of subcellular entities [? ? ? ? ?], single cells [? ? ? ?], cell assemblies [? ? ? ? ?] and even groups of animals [? ?]. This is done by extending equilibrium descriptions of condensed matter systems using broken continuous symmetries and conservation laws to certain non-equilibrium scenarios which are also well suited for describing *biological functions* like the transport of matter at scales larger than the individual active particles.

An example of active matter is provided by the coordinated beating in systems of cilia and flagella [? ?], which transport fluid. This requires *synchronization* [?], a dynamical phenomenon involving cyclic (oscillating) elements that collectively move in unison [? ? ? ?]: the simplest non-trivial broken continuous symmetry involving the temporal variable [? ? ? ?]. Biological systems that synchronize include spiking neural networks [?], and motile cells that coordinate the activity of their protruding edges to achieve net motion [?]. Another example is the structural order in the registry of microsarcomers, which constitute cardyomyocites [?] essential for the functionality of the beating heart. Similarly, collections of motors proteins [?], synchronize to achieve coordinated force generation [? ?].

However, no two aggregates of molecular motors are alike [?], just as no two neurons are identical. This variability is generic to all biological systems [?] and it is an important question how wide the variability of components can be before collective behavior is disrupted and biological function compromised.

In this article we address this question by studying synchronization of cyclic elements which we model as *non-identical* oscillators, their variability being described by stochastic frequencies which can fluctuate both within the ensemble (population variability) and also in the course of time (temporal disorder). Both of these new features aim to capture the biological population variability described above and the latter implies that periodic oscillations are replaced by generic cyclical dynamics. Our main conclusion is that breakdown of coherent motion due to population disorder is determined not by the width of the distribution about the average member (variance) but rather by the most atypical members (tails of the distribution).

An important example motivating our theoretical analysis concerns the variability of ciliary beat frequency that is observed in systems of cilia with diseases [?]. Other concrete examples are provided by sub-cellular elements like assemblies of motors proteins, or the distribution of lengths in actomyosin assemblies, where either the step or the lengths of actin filaments can vary within the assembly and can also vary, for a given element, in the course of time.

Our model describes a collection of N active elements undergoing cyclical dynamics. For simplicity our active

units are characterized by a one-dimensional spatial degree of freedom x_n. This can be thought of as the centre of mass of a flagellum [**?**] or the head of a motor protein and are subjected to active forces $f_n(t)$ which drive their motion, via $\dot{f}_n \neq 0$, for $n = 1 \ldots N$. The dynamics of x_n is obtained from the force balance following from Newton's second law associated with the evolution of forces which we generically write as

$$\rho\ddot{x}_n \approx -\gamma\dot{x}_n + f_n(t) + \sum_{m\neq n} \mathcal{I}_{nm}\,; \quad \dot{f}_n = \mathcal{F}(x_n, f_n) \quad (1)$$

For colloidal particles, such as cilia and flagella, we can safely neglect inertial terms ($\rho\ddot{x}_n \approx 0$). The first term at rhs of the first equation is a dissipative contribution, where γ is a generic friction coefficient. In the following we shall consider a well defined situation where the variables x_n perform small oscillations from an average position and as a result different particles interact weakly with each other. $\mathcal{I}_{nm}$ encodes interactions between particles at different locations $m \neq n$. Generically a sum of viscous, L and elastic, $\mathcal{J}$ couplings, (see Supplemental Material (S. M.)), $\mathcal{I}_{nm} = L_{nm}\dot{x}_m - \mathcal{J}_{nm}x_m$, it depends on both velocities and forces (proportional to deformations, x_m). For concreteness, in the following we restrict ourselves to the viscous regime, $\mathcal{J}_{nm} = 0$. In the limit of weak couplings between the particles, we can solve perturbatively for $\dot{x}_n = (f_n - kx_n)/\gamma$ and obtain a closed form equation for $\dot{x}_n$. Choosing the elastic regime instead would lead to qualitatively similar dynamics, essentially replacing viscous with elastic couplings.

The second part of Eq.(1) describes how active forces evolve in time. The rhs of this equation can be expanded w.l.g as a double power series in x_n, f_n, which for identical elements has constant coefficients, independent of n. Terms with even powers describe oscillating quantities which average to zero while odd powers give a finite contribution

$$\mathcal{F}(x_n, f_n) \sim -\kappa x_n + \mu f_n - \mu f_n x_n^2 + \alpha x_n^3 \quad (2)$$

This expansion is valid close to the oscillatory instability [**?**] and provides a universal model for stable spontaneous oscillations that can display synchronized behaviour [**?**] [**?**].

In general, $\kappa > 0$ and determines the oscillators frequency $\omega_0 := (\kappa/\gamma)^{\frac{1}{2}}$ while $\mu > 0$ is needed for stable oscillations. $T_0 := (2\pi)/\omega_0$ is the oscillation period. The sign of α is not fixed a priori. It is known that this term helps oscillators synchronize more efficiently [**?**]. Here, we choose $\alpha > 0$ which promotes in-phase synchronization in the absence of noise [**?**]. We will study the effect of noise on the phase synchronization and its loss which are summarized in the phase diagram of Fig.2.

We call 'population variability' the ensemble fluctuations which can also vary in time, resulting in temporal disorder. The simplest way to incorporate them in the model is by adding a stochastic term ϵ_n to κ. For simplicity here we restrict ourselves to a uniform distribution characterised by $\langle\epsilon_n(t)\rangle = 0$ and $\langle\epsilon_n(t)\epsilon_n(t')\rangle = \sigma^2 e^{-|t-t'|/\mathcal{T}}$. The stochastic frequency of oscillator n is $\omega_n := ([\kappa + \epsilon_n(t)]/\gamma)^{\frac{1}{2}}$.

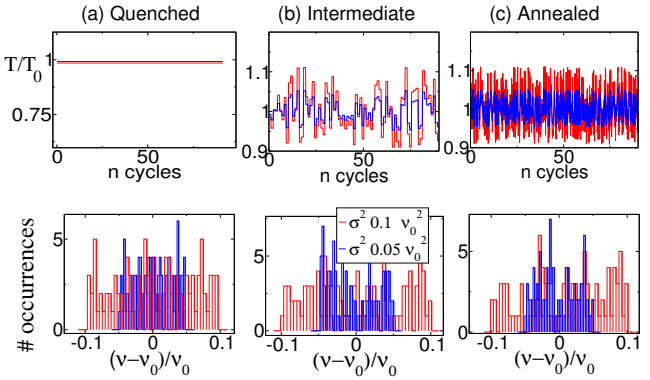

FIG. 1. Characterisation of oscillators with random components of the frequency. (a), (b) and (c) describe respectively quenched, intermediate and annealed temporal disorder. The two different colors describe two choices of noise strength, (population variability): blue lines describe deviations from the average frequency $\nu_0 = T_0^{-1}$ with a variance of $\sigma^2 = 0.05\nu_0^2$ while red lines have a variance $\sigma^2 = 0.1\nu_0^2$, where T_0 is the period of the unperturbed oscillations. Top panel: illustration of the temporal disorder showing the temporal evolution of the period of oscillation T, for an individual oscillator, in the course of time for approximatively 90 cycles. Bottom panel: population variability i.e. distributions of the oscillation frequencies ν, related to the oscillation period as $\nu := T^{-1}$, across the oscillators chain (comprising $N = 100$ oscillators) at a given instant of time (during the $50th$ cycle). Despite having different temporal evolution, all the instantaneous distributions look similar.

As a result, this active cyclic system has an intrinsic timescale given by the average oscillation period T_0 and another timescale $\mathcal{T}$ describing the time variation of the noise $\epsilon_n(t)$, or temporal disorder. In the following we shall focus on three distinct regimes for the temporal disorder: (I) $\mathcal{T} \gg T_0$, where $\epsilon_n(t)$ is a constant over many periods T_0 and the random perturbation is quenched; (II) $\mathcal{T} \ll T_0$, where $\epsilon_n(t)$ varies on a timescale much shorter than T_0 and the random perturbation can be viewed as annealed noise; (III) $\mathcal{T} \sim T_0$ where $\epsilon_n(t)$ varies on timescales of the order of the period T_0. We call this last regime an 'intermediate temporal disorder'. Quenched and annealed disorder, the limits (I) and (II), are well known [**?** **?**]; while the intermediate regime (III) has been less studied, but is particularly relevant for systems such as oscillators with an intrinsic timescale. The difference between (I),(II) and (III) is evident in the time evolution of the period of an individual oscillator, schematically illustrated respectively in the top panels of Fig.1(a),(c) and (b).

A convenient way of describing the collective synchronization dynamics considers slowly varying amplitude R_n and phase ϕ_n of oscillation, using complex variables [**?** **?**] $A_n = R_n e^{i\phi_n}$ that are related to positions $x_n(t)$, and forces, $f_n(t)$, via $x_n(t) = \frac{A_n e^{i\omega_n t}}{2} + c.c.$; and

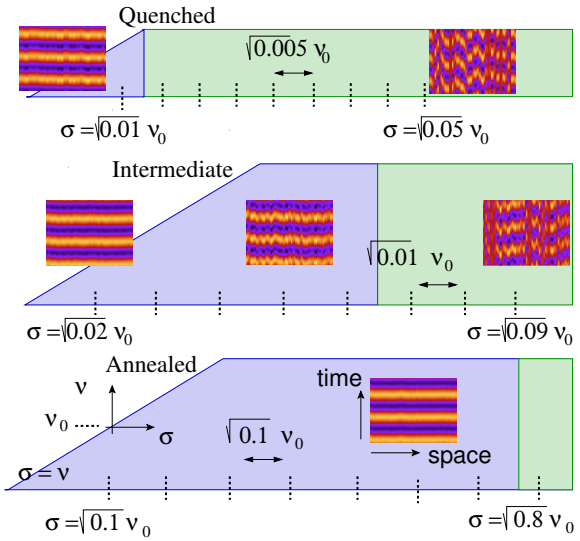

FIG. 2. Phase diagram of in-phase synchronization (blue) and loss of synchronization (green) in the plane (σ, ν) describing the standard deviation of the noise in the oscillators' frequency, σ, vs. frequency, ν. Values of σ considered in our numerics, see Fig.4, are indicated. The value of ν is drawn from a uniform distribution around $\nu_0 = T_0^{-1}$ as shown in Fig.1. (Note that σ must lie below the diagonal line $\sigma = \nu$ to ensure the actual oscillator frequency is positive.) The synchronization transition takes place at different values of σ for the different noise types: occurring first for quenched disorder, then for intermediate temporal disorder, and lastly for systems with annealed disorder which tolerate the highest level of noise. These phase boundaries can be rationalized by inspecting the eigenvalues of deterministic and random matrices associated with this dynamical system, see Fig.4. Insets: space-time plots of the phases of the oscillators (with oscillator position on the x-axis and time on the y-axis). Synchronized states yield horizontal bands while disordered patterns correspond to loss of synchrony.

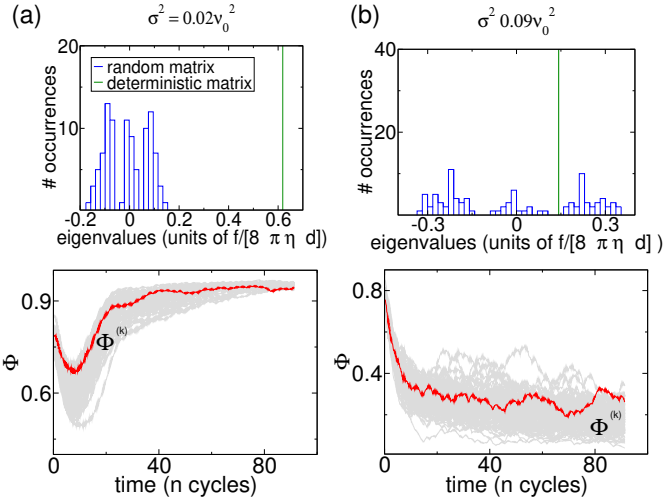

FIG. 3. Connection between synchronization and random matrices. Two examples, for the case of intermediate temporal disorder, showing the maximum eigenvalue of the deterministic matrix and the maximum eigenvalue distribution of the associated random matrix for two values of variance of noise in the oscillator frequencies: (a) $\sigma^2 = 0.02\nu_0^2$ where the system is synchronized, and (b) $\sigma^2 = 0.09\nu_0^2$, where synchronization is lost (the phase diagram is the mid panel of Fig.2). The time evolution of the order parameter Φ – defined for each realization k of the phases $\phi_n^{(k)}$ as in the Kuramoto model, $\Phi^{(k)} = \sum_n e^{i\phi_n^{(k)}}/N$ – is also shown for several realisations of the process with n labelling oscillators along the chain. Even before a transition to disorder is reached, i.e. before the order parameter goes to zero, fluctuations in the frequency induce large fluctuations in the order parameter.

$f_n(t) = i\gamma\frac{\omega_n A_n e^{i\omega_n t}}{4} + c.c.$ Here $c.c.$ indicates the complex conjugate.

Dynamical equations for f_n and x_n translate into equations for A_n that are derived using time averaging [**?** **?**]. In the present case, analytical methods can be employed only for quenched disorder where the terms ϵ_m, ϵ_n can be treated as constant on the timescale of the order of the period T_0. Writing forces and displacements in terms of complex amplitudes, $L_{nm} = \gamma^2 H_{nm}$ and approximating $H_{nm} \approx H_{nm}^{(0)} := (2\pi\eta|n-m|d)^{-1}$, valid for small oscillations, in Eq.(1), the time average of the part involving noise can be computed, giving an equation of the form [**?**]

$$\dot{A}_n = [\zeta - i\Delta_n]A_n - (\beta + i\chi)A_n|A_n|^2 + \omega_m M_{nm} A_m;$$
$$M_{nm} = i\kappa\gamma H_{nm}\frac{2}{T_0(\epsilon_m - \epsilon_n)}\sin[(\frac{\epsilon_m - \epsilon_n}{2})T_0]. \qquad (3)$$

Eq.(3) is one of our main results. Here Δ_n is a stochastic correction to the frequency and generates additive noise in the equations for the phase ϕ_n, like the Kuramoto model [**?**]. However, our model also includes *multiplicative* noise, which is given by the terms $\epsilon_m - \epsilon_n$ at the second line of Eq.(3). In the limit considered here these terms are quenched random variables [**?**], which naturally emerge from the force balance coupling oscillators m and n with different frequencies. M_{nm} is thus a random matrix [**? ? ? ? ? ?**] describing the many body, coupled, dynamics of the oscillators. The oscillators are coupled via random matrices also in the other regimes of annealed noise and intermediate noise discussed above. However in those cases the random matrix varies in time, due to the character of noise terms, and analytical approaches to derive the analogue of Eq.(3) are not feasible.

Eq.(3) provides a simple argument for understanding qualitatively the effect of noise but is not suited for a quantitative treatment, for a number of reasons. First, this approximate description works well for quenched disorder - where time averages can be taken treating noise terms as constant - but does not apply to the other regimes where the noise varies in time (annealed or intermediate temporal disorder). Second, this approach requires a reference frame which is co-rotating with all the oscillators. Specifically, in the synchronized state

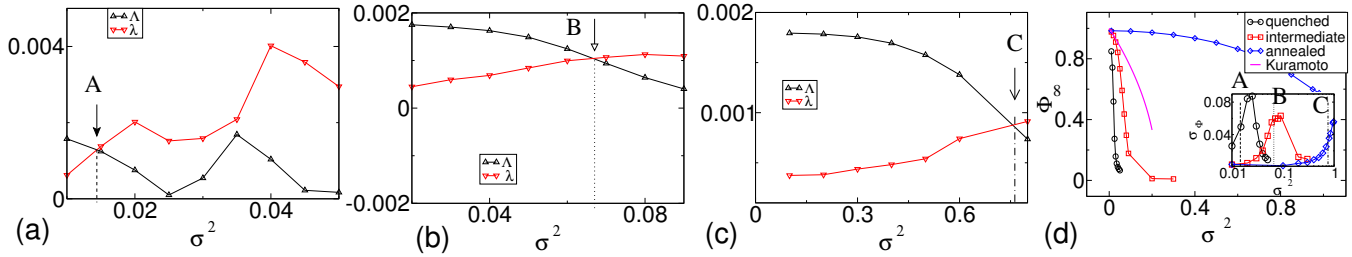

FIG. 4. Random matrix eigenvalues are good predictors for the of loss of synchronization (order-disorder transition). (a) (b) and (c) describe the trend of both the maximum deterministic eigenvalue, Λ, (black, triangles up) and of the maximum random eigenvalue, λ (red, triangles down), respectively for quenched, intermediate and annealed temporal disorder. We observe the generic trend in which Λ decreases and λ increases with increasing noise variance σ^2, except for (a) where deviations are possibly fluctuations due to the quenched system being non-self-averaging. The points where the two curves (black with triangles up and red with triangles down) cross determine the phase boundaries shown in Fig.3. (d) Order parameter Φ_∞ obtained as average over many realizations at long time. (Black) circles , (red) squares and (blue) diamonds correspond to quenched, intermediate and annealed disorder. The analytical estimate from the Kuramoto's model estimated using our parameters (details in S.M.) is also shown as a continuous (magenta) line. The inset shows the susceptibility σ_Φ measured in the numerics. Our theory predicts that synchronization is lost when $\lambda = \Lambda$, indicated by (black) dashed, dotted and dashed-dotted lines A, B and C, which anticipate the peaks of the susceptibility.

real amplitudes $R_n(t)$ relax to a constant value and and phases of oscillation $\phi_n(t)$ rotate uniformly as $\phi_n(t) \sim \Omega t$ for some Ω. Such a reference frame is not a good choice if one is interested in describing loss of synchronization due to a population variability of frequencies, which would require instead a whole population of different rotating frames. It is then more convenient to work with the equations for the real variables describing forces and positions $f_n(t), x_n(t)$ each of which oscillates about a zero value.

The calculation from this point cannot be done using analytical methods so we proceeded by numerically integrating the equations of motion for the interacting oscillators (see details in S. M.). The results presented here are for $N = 100$ oscillators studying $K = 100$ independent realizations of the noise $\epsilon_n(t)$ for either quenched, annealed, or intermediate disorder. This choice of N is motivated by the fact that many biological assemblies (such as flagella, and motors bundles) usually involve relatively small numbers of particles. We have tested the effect of increasing N (see S.M.) and find our results do not change. As the coupling terms in Eq.(1) depend on time-dependent forces $f_m(t) \sim \sin(\omega_m t + \phi_n(t))$ which in turn depend on the noise, the interaction terms are still described by random matrices whose elements we obtain numerically. To extract non-oscillating contributions, we multiply these coupling terms by $\sin(\omega_0 t)$ hence take the time-averages over the period T_0 defining new matrix elements h_{nm}

$$h_{nm} := \frac{1}{T_0}\int_0^{T_0} dt \sin(\omega_0 t) H_{nm}(t) f_m(t). \qquad (4)$$

However, h_{mn} in Eq.(4) still depend on the noise realizations. Averaging each of the matrix elements, over the K realizations we obtain (i) one single deterministic matrix $\overline{h}$, with matrix elements $\overline{h}_{mn} := \langle h_{mn} \rangle$, and (ii) K different random matrices $\delta h^{(k)}$, whose elements are $\delta h^{(k)}_{mn} := \overline{h}_{mn} - h_{mn}$ for $k = 1, \dots K$ and include both population variability and temporal disorder.

We diagonalize the matrices $\overline{h}$ and $\delta h^{(k)}$ and obtain the N eigenvalues of the deterministic matrix as well as the largest eigenvalue of each of the K random matrices. Examples of the distribution of these eigenvalues are shown in the top panels of Fig.3, using histograms (blue). For comparison, we also show a single vertical (green) line corresponding to the largest eigenvalue of the deterministic matrix $\overline{h}$. We introduce Λ, the largest eigenvalue of the deterministic matrix, $\overline{h}$, and λ_k, the largest eigenvalues of each random matrix $\delta h^{(k)}$. Furthermore, we define $\lambda := max[\lambda_k], k \in [1, K]$. Insight can be gained by studying just two oscillators (see S.M.). There in-phase synchronization occurs only when the stochastic contribution is smaller than the deterministic one. For the N-particle system, the condition for synchronization is $\Lambda > \lambda$. If fluctuations become strong enough, i.e. when $\Lambda < \lambda$, they overcome deterministic dynamics and synchronization is lost. Hence the loss of synchronization occurs at the critical value [**?**] $\Lambda = \lambda_c$ which can be identified by looking at the distribution of the largest eigenvalue of the random matrix [**? ? ? ? ? ?**]. This is observed numerically, and the intersection points where λ and Λ cross in Fig.4(a),(b),(c) define the boundaries in the phase diagram of Fig.2. To characterize the transition, we study also the susceptibility $\sigma_\Phi := \sum_{k=1}^{K} (\Phi_\infty^{(k)} - \Phi_\infty)^2 / K$, where $\Phi_\infty^{(k)} = \Phi^{(k)}(t \gg T_0)$ is the order parameter in the k-th realization at sufficiently long time, defined as $\Phi^{(k)}(t) := \frac{1}{N}\sum_n e^{i\phi_n^{(k)}(t)}$ [**?**] (see Fig.3 where specific realizations of the order parameters are highlighted in red), and $\Phi_\infty := \sum_{k=1}^{K} \Phi_\infty^{(k)} / K$ is the average over many realizations. Loss of synchronization predicted from the theoretical analysis on the critical value λ_c of the random matrix largest eigenvalue – see the points A, B, C associated to the vertical dashed,

dotted and dash-dotted lines in Fig.4 – anticipates the peaks in the susceptibility obtained from numerics, inset of Fig.4(c). The peaks occur at larger values of the noise strength. This suggests that the susceptibility, which is associated to the variance and measures the width of the distribution, is not adequate for characterizing this type of transition which is controlled instead by the most atypical members of the population.

In conclusion, we addressed a broad question: how variable a collection of active mechanical elements can be before their coherent motion, and their *biological functionality*, are disrupted. To answer to this question we studied cyclic active elements possessing one oscillating degree of freedom. The system's variability is due to fluctuations in the frequency, which can vary both across the population and in the course of time. In systems of particles with pairwise interactions, oscillations with fluctuating frequency are propagated mechanically to all other particles. This results in multiplicative noise terms that can be described with random matrices. Such an observation revealed a surprising and interesting connection to the well known fact that the largest eigenvalue of a random matrix controls the stability of the associated random dynamical system. Hence the development of coherent motion is dominated by the properties of the tail of the probability distribution of the eigenvalues. We envisage a similar scenario when the framework of active matter is applied to other realistic biological problems. A concrete realization of our model is in the context of cilia where coordinated movements serve for transport. Its failure, associated to a large variability in the cilia beat frequencies, results in diseases like bronchiectasis [**?**]. Another example can be found when inhomogeneities in the fluid/gel (mucus) directly affect the mechanical coupling of nearby cilia which might lead to malfunctioning and diseases such as cystic fibrosis [**?**]. Similar losses of functionality might be observed also with experiments involving motor proteins in vitro [**?**] if chemical fuel (ATP) is not homogeneously distributed in space and time.

ACKNOWLEDGMENTS

M.L. acknowledges financial support from the ICAM Branch Contributions and Labex Celtisphybio N^o ANR-10-LBX-0038 part of the IDEX PSL N^o ANR-10-IDEX-0001-02 PSL. T.B.L. acknowledges the support of BrisSynBio, a BBSRC/EPSRC Synthetic Biology Research Centre, grant number BB/L01386X/1.